



基于重构边界光滑离散剪切间隙法的复合材料层合板自由振动分析

李 情，陈莘莘

Free Vibration Analysis of Laminated Composite Plates Based on the Reconstructed Edge-Based Smoothing DSG Method

LI Qing and CHEN Shenshen

在线阅读 View online: <https://doi.org/10.21656/1000-0887.430109>

您可能感兴趣的其他文章

Articles you may be interested in

基于n阶剪切变形理论的复合材料层合板屈曲分析

Buckling Analysis of Composite Laminate Plates Based on the n-order Shear Deformation Theory

应用数学和力学. 2020, 41(12): 1346–1357 <https://doi.org/10.21656/1000-0887.410061>

弹性约束边界条件下矩形蜂窝夹芯板的自由振动分析

Free Vibration Analysis of Rectangular Honeycomb-Cored Plates Under Elastically Constrained Boundary Conditions

应用数学和力学. 2019, 40(6): 583–594 <https://doi.org/10.21656/1000-0887.390348>

任意弹性边界的多段梁自由振动研究

Free Vibration of MultiSegment Beams With Arbitrary Boundary Conditions

应用数学和力学. 2020, 41(9): 985–993 <https://doi.org/10.21656/1000-0887.410045>

悬索桥竖向自由振动的传递矩阵解

A Transfer Matrix Algorithm for Vertical Free Vibration of Suspension Bridges

应用数学和力学. 2019, 40(9): 991–999 <https://doi.org/10.21656/1000-0887.390221>

基于4变量精确平板理论的剪切效应分析

Shear Effect Analysis on Plates Based on the 4-Variable Refined Plate Theory

应用数学和力学. 2018, 39(11): 1268–1281 <https://doi.org/10.21656/1000-0887.390066>

双功能梯度纳米梁系统振动分析的辛方法

A Symplectic Approach for Free Vibration of Functionally Graded Double-Nanobeam Systems Embedded in Viscoelastic Medium

应用数学和力学. 2018, 39(10): 1159–1171 <https://doi.org/10.21656/1000-0887.390130>



关注微信公众号，获得更多资讯信息

基于重构边界光滑离散剪切间隙法的 复合材料层合板自由振动分析^{*}

李 情, 陈莘莘

(华东交通大学 土木建筑学院, 南昌 330013)

摘要: 重构边界光滑离散剪切间隙(RES-DSG3)法, 利用边界光滑技术将域积分转化为沿光滑域边界的边界积分, 结合基于全局坐标系的非等参离散剪切间隙(DSG)法, 避免了坐标映射和 Jacobi 矩阵的计算, 同时克服了“剪切自锁”现象, 提高了计算的精度。基于一阶剪切变形理论, 采用该文给出的方法, 从不同材料参数、边厚比、边界条件等几个方面对复合材料层合板自由振动固有频率进行了数值分析, 通过典型算例的计算, 验证了该方法的可行性和有效性。

关 键 词: 边界光滑技术; 离散剪切间隙; 复合材料层合板; 一阶剪切变形理论; 自由振动

中图分类号: O242; O343 文献标志码: A DOI: 10.21656/1000-0887.430109

Free Vibration Analysis of Laminated Composite Plates Based on the Reconstructed Edge-Based Smoothing DSG Method

LI Qing, CHEN Shenshen

(School of Civil Engineering and Architecture, East China Jiaotong University, Nanchang 330013, P.R.China)

Abstract: To avoid transverse shear locking and improve the accuracy, the RES-DSG3 method was proposed through the incorporation of the non-isoparametric DSG method with a novel edge-based smoothing technique based on global coordinates, and all the integration of smoothed matrices can be calculated along the boundary segments of smoothed cells without coordinate mapping. Based on the 1st-order shear theory, the RES-DSG3 method was used to analyze free vibration natural frequencies of laminated composite plates with different material parameters, edge-thickness ratios and boundary conditions. The free vibrations of the composite plates were analyzed numerically. The calculation of the example verifies the feasibility and effectiveness of the proposed method.

Key words: edge-based smoothing technique; discrete shear gap; laminated composite plate; 1st-order shear deformation theory; free vibration

引 言

复合材料层合结构因其比强度高、耐高温耐腐蚀、比模量高、可设计性好等优点, 广泛用于航空航天、汽

* 收稿日期: 2022-03-31; 修订日期: 2022-06-22

基金项目: 国家自然科学基金(12172131; 11772129)

作者简介: 李情(1986—), 女, 讲师, 硕士(E-mail: liqing_726@163.com);

陈莘莘(1975—), 男, 教授, 博士(通讯作者. E-mail: chenshenshen@tsinghua.org.cn).

引用格式: 李情, 陈莘莘. 基于重构边界光滑离散剪切间隙法的复合材料层合板自由振动分析[J]. 应用数学和力学, 2022, 43(10): 1123-1132.

车、船舶海洋等工程领域,对其振动特性的研究具有重要的工程意义^[1-3].现有层合板理论的主要差别是对于横向剪切形变的处理,经典层合理论基于 Kirchhoff-Love 假设,忽略了层间的剪切和挤压,只适用于薄板;一阶剪切变形理论(FSDT)考虑横向剪切形变,引入了剪切修正系数,对中厚板适用结果良好;高阶剪切变形板理论(HSDT)引入剪切应力沿板厚方向的非线性变化,避免了 FSDT 剪切修正系数的引入,但是需要有限元方程 C¹ 连续,在实际计算过程中较难实现.诸多学者利用较为简洁的 FSDT 对层合板进行了自由振动分析,得到了令人满意的结果.

迄今为止,工程结构分析中常见的数值计算方法有:有限元法、边界元法、无网格法等.作为应用最为广泛和成熟的数值计算方法,有限元法在复合材料层合板的动力问题分析中应用广泛^[4-5].然而,传统的有限元法大多是基于自然坐标的,计算时需要进行等参变换和 Jacobi 矩阵的计算,当单元严重不规则或变形时,坐标转换的要求将显著降低计算精度;同时,刚度矩阵存在过刚现象,对三角形单元等低阶单元尤为突出.为了解决上述难点,学者们提出了不同的解决方法,Liu 等^[6] 将有限元法和无网格法中的应变光滑技术相结合,提出了光滑有限元法(S-FEM),展现了良好的计算精度、效率和稳定性.基于光滑域构造方式的不同,光滑有限元法包括基于单元子域的光滑有限元法(CS-FEM)^[6]、基于单元节点的光滑有限元法(NS-FEM)^[7]、基于单元边界的光滑有限元法(ES-FEM)^[8] 和基于单元面的光滑有限元法(FS-FEM)^[9].众多学者将光滑有限元法拓展到弹塑性问题^[10-11]、板壳问题^[12-13] 以及复合材料分析^[14-15] 等领域,并取得了良好的结果.目前 Reissner-Mindlin 板壳单元依然是工程实际数值计算中常见的单元类型,但当板壳厚度很薄时,常伴随“剪切自锁”的现象.为了消除自锁,众多学者开展了大量的研究工作,提出了不同的解决方法,比如基于选择性积分的板壳单元、MITC4 单元、C0 单元、EAS 单元、ANS 单元等.Bletzinger 等^[16] 提出了离散剪切间隙(DSG)法,构造了 DSG3 单元,利用离散单元剪切间隙得到新的剪切应变矩阵,削弱了“自锁”现象.然而,原始 DSG 单元的剪切应变会受单元节点编号的顺序变化的影响,尤其是对于不规则网格和畸变网格,计算精度和稳定性不高.

Nguyen-Xuan 和 Nguyen-Thoi 等将光滑有限元法与 DSG 法结合,提出了 ES-DSG3 单元^[17]、NS-DSG 单元^[18]、CS-DSG 单元^[12],用于分析 Reissner-Mindlin 板的问题,得到了较好的结果.值得注意的是,在上述方法中虽然对应变矩阵进行了光滑处理,但是 Reissner-Mindlin 板有限元方程中的荷载矢量、质量矩阵仍需要进行等参变换,无法完全避免坐标映射和变换.由此,Yang 等^[19] 基于全局坐标构造了 Reissner-Mindlin 板改进的边界光滑 DSG 单元(RES-DSG3),提出了一种非等参 DSG 方法,将其与符号积分和光滑技术相结合,对矩阵进行了光滑处理,同时避免了坐标映射,并将此法用于分析 Reissner-Mindlin 板,取得了良好的计算结果.本文借助于 RES-DSG3 法,详细推导了复合材料层合板自由振动的控制方程,并编制了相应的 MATLAB 程序,通过典型算例的计算,验证了本文方法的可行性和有效性.

1 层合板自由振动的有限元控制方程

基于 FSDT,复合材料层合板的位移场可以描述为

$$\begin{aligned} u(x, y, z) &= u_0(x, y) + z\beta_x(x, y), \\ v(x, y, z) &= v_0(x, y) + z\beta_y(x, y), \\ w(x, y, z) &= w_0(x, y), \end{aligned} \quad (1)$$

式中, u, v, w 表示层合板内任意点 x, y, z 变形后的位移, u_0, v_0, w_0 表示层合板中面上相应点的位移, β_x, β_y 为中面法线关于 y 轴和 x 轴方向的转角,如图 1 所示.

位移应变关系为

$$\left\{ \begin{array}{l} \varepsilon_{xx} \\ \varepsilon_{yy} \\ \gamma_{xy} \end{array} \right\} = \left\{ \begin{array}{l} \frac{\partial u_0}{\partial x} \\ \frac{\partial v_0}{\partial y} \\ \frac{\partial u_0}{\partial y} + \frac{\partial v_0}{\partial x} \end{array} \right\} + z \left\{ \begin{array}{l} \frac{\partial \beta_x}{\partial x} \\ \frac{\partial \beta_y}{\partial y} \\ \frac{\partial \beta_x}{\partial y} + \frac{\partial \beta_y}{\partial x} \end{array} \right\} = \boldsymbol{\varepsilon}_0 + z\boldsymbol{k}, \quad (2)$$

$$\begin{Bmatrix} \gamma_{xz} \\ \gamma_{yz} \end{Bmatrix} = \begin{Bmatrix} \beta_x + \frac{\partial w_0}{\partial x} \\ \beta_y + \frac{\partial w_0}{\partial y} \end{Bmatrix} = \boldsymbol{\gamma}_0. \quad (3)$$

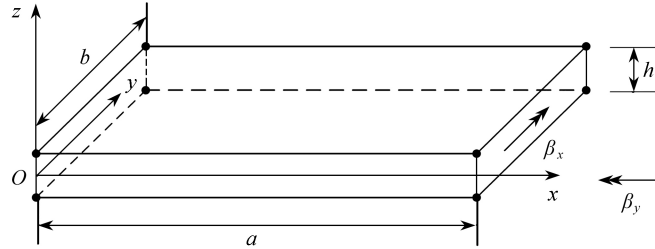


图 1 层合板的坐标系
Fig. 1 The coordinate system for the laminate

合力、合力矩和等效剪力向量可分别描述为

$$\mathbf{N} = (N_x \ N_y \ N_{xy})^T, \mathbf{M} = (M_x \ M_y \ M_{xy})^T, \mathbf{Q}_s = (Q_x \ Q_y)^T. \quad (4)$$

则广义本构关系为

$$\begin{Bmatrix} \mathbf{N} \\ \mathbf{M} \\ \mathbf{Q}_s \end{Bmatrix} = \begin{Bmatrix} \mathbf{A} & \mathbf{B} & 0 \\ \mathbf{B} & \mathbf{D} & 0 \\ 0 & 0 & \mathbf{A}_s \end{Bmatrix} \begin{Bmatrix} \boldsymbol{\varepsilon}_0 \\ \boldsymbol{k} \\ \boldsymbol{\gamma}_0 \end{Bmatrix} = \begin{Bmatrix} \bar{\mathbf{D}} & 0 \\ 0 & \mathbf{A}_s \end{Bmatrix}, \quad (5)$$

式中, \mathbf{A} 为拉伸刚度矩阵, \mathbf{B} 为耦合刚度矩阵, \mathbf{D} 为弯曲刚度矩阵, \mathbf{A}_s 为剪切刚度矩阵, 它们的元素可以分别表示为

$$\mathbf{A} = \begin{bmatrix} A_{11} & A_{12} & A_{16} \\ A_{21} & A_{22} & A_{26} \\ A_{61} & A_{62} & A_{66} \end{bmatrix}, \mathbf{B} = \begin{bmatrix} B_{11} & B_{12} & B_{16} \\ B_{21} & B_{22} & B_{26} \\ B_{61} & B_{62} & B_{66} \end{bmatrix}, \mathbf{D} = \begin{bmatrix} D_{11} & D_{12} & D_{16} \\ D_{21} & D_{22} & D_{26} \\ D_{61} & D_{62} & D_{66} \end{bmatrix}, \mathbf{A}_s = \begin{bmatrix} A_{44} & A_{45} \\ A_{45} & A_{55} \end{bmatrix},$$

其中

$$(A_{ij} \ B_{ij} \ D_{ij}) = \int_{-h/2}^{h/2} \bar{Q}_{ij}(1-z-z^2)dz = \sum_{n=1}^N \int_{z_n}^{z_{n+1}} \bar{Q}_{ij}^{(n)}(1-z-z^2)dz, \quad i, j = 1, 2, 6, \quad (6)$$

$$A_{sij} = \zeta \int_{-h/2}^{h/2} \bar{Q}_{ij}(1-z-z^2)dz = \sum_{n=1}^N \zeta \int_{z_n}^{z_{n+1}} \bar{Q}_{ij}^{(n)} dz, \quad i, j = 4, 5, \quad (7)$$

上标 (n) 表示第 n 层, \bar{Q}_{ij} 表示弹性矩阵系数, ζ 为剪切修正因子.

根据 Hamilton 原理, 不考虑阻尼, 可得层合板自由振动的有限元控制方程为

$$\mathbf{K}\mathbf{u} + \mathbf{M}\ddot{\mathbf{u}} = \mathbf{0}, \quad (8)$$

式中, \mathbf{K} 为结构的系统刚度矩阵, \mathbf{M} 为结构的系统质量矩阵, \mathbf{u} 为系统的位移矢量. 同时有

$$\mathbf{K} = \mathbf{K}^b + \mathbf{K}^s, \quad (9)$$

且

$$\mathbf{K}_{ij}^b = \int_{\Omega} (\mathbf{B}_i^b)^T \bar{\mathbf{D}} \mathbf{B}_j^b d\Omega, \quad (10)$$

$$\mathbf{K}_{ij}^s = \int_{\Omega} (\mathbf{B}_i^s)^T \mathbf{A}_s \mathbf{B}_j^s d\Omega. \quad (11)$$

\mathbf{B}_i^b 和 \mathbf{B}_i^s 的表达式分别为

$$\mathbf{B}_i^b = \begin{bmatrix} \partial N_i / \partial x & 0 & 0 & 0 & 0 \\ 0 & \partial N_i / \partial y & 0 & 0 & 0 \\ \partial N_i / \partial y & \partial N_i / \partial x & 0 & 0 & 0 \\ 0 & 0 & 0 & \partial N_i / \partial x & 0 \\ 0 & 0 & 0 & 0 & \partial N_i / \partial y \\ 0 & 0 & 0 & \partial N_i / \partial y & \partial N_i / \partial x \end{bmatrix}, \quad (12)$$

$$\mathbf{B}_i^s = \begin{bmatrix} 0 & 0 & \partial N_i / \partial x & N_i & 0 \\ 0 & 0 & \partial N_i / \partial y & 0 & N_i \end{bmatrix}, \quad (13)$$

式中, N_i 为单元的形函数.

单元的质量矩阵为

$$\mathbf{M}_{ij} = \int_{\Omega} N_i^T \mathbf{m} N_j d\Omega, \quad (14)$$

式中, \mathbf{m} 为质量密度矩阵, 其表达式为

$$\mathbf{m} = \begin{bmatrix} I_1 & 0 & 0 & I_2 & 0 \\ 0 & I_1 & 0 & 0 & I_2 \\ 0 & 0 & I_1 & 0 & 0 \\ I_2 & 0 & 0 & I_3 & 0 \\ 0 & I_2 & 0 & 0 & I_3 \end{bmatrix}. \quad (15)$$

对第 K 层材料有

$$(I_1 \ I_2 \ I_3) = \int_{z_{k-1}}^{z_k} \rho^{(k)} (1 \ z \ z^2) dz. \quad (16)$$

2 RES-DSG3 法^[17]

2.1 基于全局坐标系的非等参DSG3 法

有限元方程中节点 i 相关的剪切间隙可描述为全局卡氏坐标系下的标量形式:

$$\Delta w_{yx}^i(x, y) = \int_{x_1}^{x^i} \gamma_x^h dx = w^h(x, y) \Big|_{x_1}^{x^i} + \int_{x_1}^{x^i} \beta_x^h dx, \quad (17)$$

$$\Delta w_{yy}^i(x, y) = \int_{y_1}^{y^i} \gamma_y^h dy = w^h(x, y) \Big|_{y_1}^{y^i} + \int_{y_1}^{y^i} \beta_y^h dy, \quad (18)$$

同时

$$\Delta N_j^{xi} = N_j(x_i, y) - N_j(x_1, y), \quad (19)$$

$$\Delta N_j^{yi} = N_j(x, y_i) - N_j(x, y_1). \quad (20)$$

全局坐标系下, 三角形单元的形函数为

$$\mathbf{N} = (1 \ x \ y) \begin{bmatrix} 1 & x_1 & y_1 \\ 1 & x_2 & y_2 \\ 1 & x_3 & y_3 \end{bmatrix}^{-1} = (1 \ x \ y) \begin{bmatrix} a_{11} & a_{12} & a_{13} \\ a_{21} & a_{22} & a_{23} \\ a_{31} & a_{32} & a_{33} \end{bmatrix} = \mathbf{P}_{T3} \mathbf{A}_{T3}, \quad (21)$$

式中, x_i, y_i 为三角形单元节点的全局坐标, a_{ij} ($i=1, 2, 3; j=1, 2, 3$) 是与式 (21) 中逆矩阵对应的矩阵元素.

将形函数代入方程 (17)、(18), 得到

$$\Delta w_{yx}^i(x, y) = \Delta \hat{\mathbf{N}}^{xi} \hat{\mathbf{w}} + \bar{\mathbf{N}}^{xi} \hat{\boldsymbol{\beta}}_x, \quad (22)$$

$$\Delta w_{yy}^i(x, y) = \Delta \hat{\mathbf{N}}^{yi} \hat{\mathbf{w}} + \bar{\mathbf{N}}^{yi} \hat{\boldsymbol{\beta}}_y, \quad (23)$$

式中

$$\hat{\mathbf{w}} = (w_1 \ w_2 \ w_3)^T, \quad \hat{\boldsymbol{\beta}}_x = (\beta_{x1} \ \beta_{x2} \ \beta_{x3})^T, \quad \hat{\boldsymbol{\beta}}_y = (\beta_{y1} \ \beta_{y2} \ \beta_{y3})^T, \quad (24)$$

$$\Delta \hat{\mathbf{N}}^{xi} = \hat{\mathbf{P}}_{T3x} \mathbf{A}_{T3}, \quad \hat{\mathbf{P}}_{T3x} = (0 \ x_i - x_1 \ 0), \quad (25)$$

$$\Delta \hat{\mathbf{N}}^{yi} = \hat{\mathbf{P}}_{T3y} \mathbf{A}_{T3}, \quad \hat{\mathbf{P}}_{T3y} = (0 \ 0 \ y_i - y_1), \quad (26)$$

$$\bar{\mathbf{N}}^{xi} = \bar{\mathbf{P}}_{T3x} \mathbf{A}_{T3}, \quad \bar{\mathbf{P}}_{T3x} = \left[x_i - x_1 \quad \frac{1}{2}(x_i^2 - x_1^2) \quad y(x_i - x_1) \right], \quad (27)$$

$$\bar{\mathbf{N}}^{yi} = \bar{\mathbf{P}}_{T3y} \mathbf{A}_{T3}, \quad \bar{\mathbf{P}}_{T3y} = \left[y_i - y_1 \quad x(y_i - y_1) \quad \frac{1}{2}(y_i^2 - y_1^2) \right]. \quad (28)$$

则剪切应变可表示为

$$\gamma_x = \frac{dN}{dx} \Delta w_{yx}, \quad \gamma_y = \frac{dN}{dy} \Delta w_{yy}, \quad (29)$$

$$\Delta w_{yx} = (0 \quad \Delta w_{yx}^2 \quad \Delta w_{yx}^3)^T, \quad (30)$$

$$\Delta w_{yy} = (0 \quad \Delta w_{yy}^2 \quad \Delta w_{yy}^3)^T. \quad (31)$$

基于 DSG 方程, 复合材料层合板的单元剪切应变可写为矩阵形式, 如下:

$$\boldsymbol{\gamma}_e = \begin{Bmatrix} \gamma_{ex} \\ \gamma_{ey} \end{Bmatrix} = \begin{Bmatrix} \sum_{i=1}^{N_{\text{nod}}} \frac{dN_i}{dx} \Delta w_{yx}^i \\ \sum_{i=1}^{N_{\text{nod}}} \frac{dN_i}{dy} \Delta w_{yy}^i \end{Bmatrix} = \mathbf{B}_e^{\text{DSG3}} [\mathbf{d}_1^e \quad \mathbf{d}_2^e \quad \mathbf{d}_3^e]^T, \quad (32)$$

式中

$$\mathbf{d}_i^e = (u_i^e \quad v_i^e \quad w_i^e \quad \beta_{xi}^e \quad \beta_{yi}^e)^T, \quad (33)$$

$$\mathbf{B}_e^{\text{DSG3}} = (\mathbf{B}_{ex}^{\text{DSG3}} \quad \mathbf{B}_{ey}^{\text{DSG3}})^T, \quad (34)$$

$$\mathbf{B}_{exi}^{\text{DSG3}} = \begin{pmatrix} 0 & 0 & \sum_{j=2}^3 a_{2j} \Delta \hat{N}_i^{xj} & \sum_{j=2}^3 a_{2j} \bar{N}_i^{xj} & 0 \end{pmatrix}, \quad i = 1, 2, 3, \quad (35)$$

$$\mathbf{B}_{eyi}^{\text{DSG3}} = \begin{pmatrix} 0 & 0 & \sum_{j=2}^3 a_{2j} \Delta \hat{N}_i^{yj} & \sum_{j=2}^3 a_{2j} \bar{N}_i^{yj} & 0 \end{pmatrix}, \quad i = 1, 2, 3. \quad (36)$$

2.2 边界光滑技术

对于平面问题, 基于符号积分和 Gauss 散度定理有

$$\int_{\Omega^s} f(x, y) d\Omega = \int_{\Gamma^s} \left(\int f(x, y) dx \right) n_x d\Gamma, \quad (37)$$

$$\int_{\Omega^s} f(x, y) d\Omega = \int_{\Gamma^s} \left(\int f(x, y) dy \right) n_y d\Gamma, \quad (38)$$

式中, Γ 为积分域边界.

假设积分域包含 k 条边界, 且为光滑连续, 则式 (37)、(38) 可写为沿积分域边界的线积分之和:

$$\int_{\Omega^s} f(x, y) d\Omega = \sum_{i=1}^k \int_{\Gamma_i^s} \left(\int f(x, y) dx \right) n_x^i d\Gamma, \quad (39)$$

$$\int_{\Omega^s} f(x, y) d\Omega = \sum_{i=1}^k \int_{\Gamma_i^s} \left(\int f(x, y) dy \right) n_y^i d\Gamma, \quad (40)$$

式中, n_x^i, n_y^i 为 Γ_i^s 与 x, y 轴之间的夹角的方向余弦.

应用近似积分技术, 光滑域内点 x_C 处的任意函数可表示为

$$\tilde{f}(x_C) = \int_{\Omega^s} f(x) \phi(x - x_C) d\Omega, \quad (41)$$

式中, $\phi(x - x_C)$ 为光滑函数, 定义为

$$\phi(x - x_C) = \begin{cases} 1/A_C, & x \in \Omega^s, \\ 0, & x \notin \Omega^s, \end{cases} \quad (42)$$

其中 $A_C = \int_{\Omega^s} d\Omega$ 为单元 Ω_e 中的光滑域 Ω_C 的面积.

将式 (42) 代入式 (41) 中, 得

$$\tilde{f}(x_C) = \frac{1}{A_C} \int_{\Omega^s} f(x) d\Omega. \quad (43)$$

将式 (43) 代入式 (39)、(40) 中, 得

$$\tilde{f}(x_C) = \frac{1}{A_C} \int_{\Omega^s} f(x) d\Omega = \frac{1}{A_C} \sum_{i=1}^k \int_{\Gamma_i^s} \left(\int f(x) dx \right) n_x^i d\Gamma, \quad (44)$$

$$\tilde{f}(x_C) = \frac{1}{A_C} \int_{\Omega^s} f(x) d\Omega = \frac{1}{A_C} \sum_{i=1}^k \int_{\Gamma_i^s} \left(\int f(x) dy \right) n_y^i d\Gamma. \quad (45)$$

引入 Gauss 积分, 得

$$\tilde{f}(x_C) = \frac{1}{A_C} \int_{\Omega^s} f(x) d\Omega = \frac{1}{A_C} \sum_{i=1}^k \sum_{j=1}^{N_G} \frac{1}{2} W_{i,j} \varphi_x(x_{x,j}^{\text{GP}}) n_x^i l_i, \quad (46)$$

$$\tilde{f}(x_C) = \frac{1}{A_C} \int_{\Omega^s} f(x) d\Omega = \frac{1}{A_C} \sum_{i=1}^k \sum_{j=1}^{N_G} \frac{1}{2} W_{i,j} \varphi_y(x_{y,j}^{\text{GP}}) n_y^i l_i, \quad (47)$$

同时

$$\varphi_x(x_{x,j}^{\text{GP}}) = \left(\int f(x) dx \right) \Big|_{x_{x,j}^{\text{GP}}}, \quad \varphi_y(x_{y,j}^{\text{GP}}) = \left(\int f(x) dy \right) \Big|_{x_{y,j}^{\text{GP}}}, \quad (48)$$

式中, $x_{x,j}^{\text{GP}}$ 为边界 Γ_i 的 Gauss 积分点, 其长度为 l_i , $W_{i,j}$ 是与 $x_{x,j}^{\text{GP}}$ 的 Gauss 积分点相对应的权系数, N_G 表示每条边界上的 Gauss 积分点的个数.

3 基于 REG-DSG3 的有限元方程

假设求解域 Ω 离散为 N_e 个单元, 求解域 $\Omega = \sum_{i=1}^{N_e} \Omega_e$, 这些单元网格共有 N_{eg} 条边, 将每条边的两个端点和这条边相邻的两个三角形单元的中心相连接, 这样就在三角形单元的基础上形成了 N_s 个基于边的光滑域, 求解域 $\Omega = \sum_{k=1}^{N_{\text{eg}}} \Omega_k$, 光滑域的数目和三角形单元边的数目相等, 即 $N_{\text{eg}} = N_s$, 如图 2 所示.

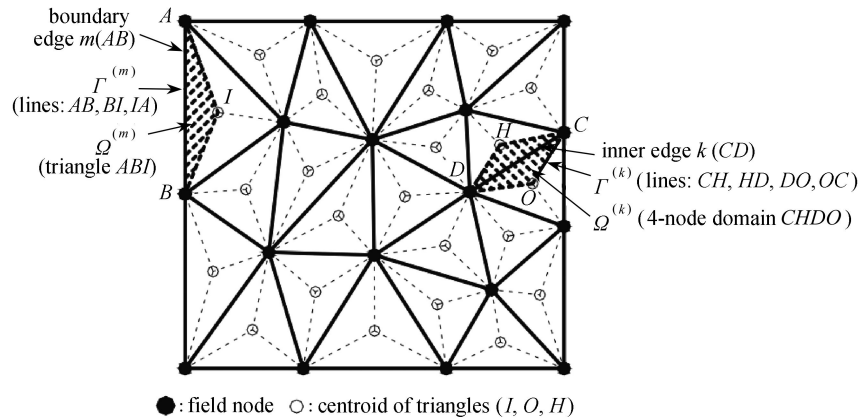


图 2 三角形单元和基于边界的光滑域
Fig. 2 Triangular elements and smoothing domains associated with edges

利用边界光滑技术和 DSG 单元, 层合板自由振动控制方程中的应变矩阵可表示为

$$\tilde{\mathbf{B}}_i^b = \frac{1}{A_C} \int_{\Gamma^s} \begin{bmatrix} N_i n_x & 0 & 0 & 0 & 0 \\ 0 & N_i n_y & 0 & 0 & 0 \\ N_i n_y & N_i n_x & 0 & 0 & 0 \\ 0 & 0 & 0 & N_i n_x & 0 \\ 0 & 0 & 0 & 0 & N_i n_y \\ 0 & 0 & 0 & N_i n_y & N_i n_x \end{bmatrix} d\Gamma = \begin{bmatrix} \tilde{b}_{ix} & 0 & 0 & 0 & 0 \\ 0 & \tilde{b}_{iy} & 0 & 0 & 0 \\ \tilde{b}_{iy} & \tilde{b}_{ix} & 0 & 0 & 0 \\ 0 & 0 & 0 & \tilde{b}_{ix} & 0 \\ 0 & 0 & 0 & 0 & \tilde{b}_{iy} \\ 0 & 0 & 0 & \tilde{b}_{iy} & \tilde{b}_{ix} \end{bmatrix}, \quad (49)$$

其中

$$\tilde{b}_{ij} = \frac{1}{A_C} \sum_{m=1}^k \sum_{n=1}^{N_G} \frac{1}{2} W_{m,n} N_i(x_{m,n}^{\text{GP}}) n_j^m l_m, \quad j = x, y, \quad (50)$$

式中, k 表示每个光滑域的边界段数, 对于求解域内边界处的边, $k=3$, 对于求解域内部的边, $k=4$; N_i 是与边界段 m 相关的三角形单元节点 i 的形函数。

$$\begin{aligned} \tilde{\mathbf{B}}_i^{\text{bDSG3}} &= \frac{1}{A_C} \int_{\Omega^s} (\tilde{\mathbf{B}}_{ix}^{\text{bDSG3}} \quad \tilde{\mathbf{B}}_{iy}^{\text{bDSG3}})^T d\Omega = \\ &\frac{1}{A_C} \int_{\Gamma^s} \left(\left(\int \tilde{\mathbf{B}}_{ix}^{\text{bDSG3}} \right) n_x \quad \left(\int \tilde{\mathbf{B}}_{iy}^{\text{bDSG3}} \right) n_y \right)^T d\Gamma = (\tilde{\mathbf{b}}_{ix}^{\text{bDSG3}} \quad \tilde{\mathbf{b}}_{iy}^{\text{bDSG3}})^T, \end{aligned} \quad (51)$$

其中

$$\tilde{b}_{ix}^{\text{b}} = \frac{1}{A_C} \sum_{m=1}^k \sum_{n=1}^{N_G} \frac{1}{2} W_{m,n} \Phi_{ix}^{\text{DSG3}}(x_{m,n}^{\text{GP}}, y_{m,n}^{\text{GP}}) n_x^m l_m, \quad (52)$$

$$\tilde{b}_{iy}^{\text{b}} = \frac{1}{A_C} \sum_{m=1}^k \sum_{n=1}^{N_G} \frac{1}{2} W_{m,n} \Phi_{iy}^{\text{DSG3}}(x_{m,n}^{\text{GP}}, y_{m,n}^{\text{GP}}) n_x^m l_m, \quad (53)$$

$$\Phi_{ix}^{\text{DSG3}}(x_{m,n}^{\text{GP}}, y_{m,n}^{\text{GP}}) = \left(0 \ 0 \ \sum_{j=2}^3 a_{2j} x \Delta \hat{N}_i^{xj} \ \sum_{j=2}^3 a_{2j} x \bar{N}_i^{xj} \ 0 \right) \Big|_{(x_{m,n}^{\text{GP}}, y_{m,n}^{\text{GP}})}, \quad (54)$$

$$\Phi_{iy}^{\text{DSG3}}(x_{m,n}^{\text{GP}}, y_{m,n}^{\text{GP}}) = \left(0 \ 0 \ \sum_{j=2}^3 a_{2j} y \Delta \hat{N}_i^{yj} \ 0 \ \sum_{j=2}^3 a_{2j} y \bar{N}_i^{yj} \right) \Big|_{(x_{m,n}^{\text{GP}}, y_{m,n}^{\text{GP}})}, \quad (55)$$

式中, $\Delta \hat{N}_i^{xj}$, $\Delta \hat{N}_i^{yj}$, \bar{N}_i^{xj} , \bar{N}_i^{yj} 的定义参见式 (25)~(28)。

由此, 光滑刚度矩阵为

$$\tilde{\mathbf{K}} = \sum_{C=1}^{N_{\text{eg}}} A_C (\tilde{\mathbf{B}}_C^{\text{b}})^T \tilde{\mathbf{D}} \tilde{\mathbf{B}}_C^{\text{b}} + \sum_{C=1}^{N_{\text{eg}}} A_C (\tilde{\mathbf{B}}_C^{\text{sDSG3}})^T \mathbf{A}_S \tilde{\mathbf{B}}_C^{\text{sDSG3}}. \quad (56)$$

同理, 光滑质量矩阵可通过以下转换得到:

$$\tilde{N}_i = \frac{1}{A_C} \int_{\Omega^s} N_i d\Omega = \frac{1}{A_C} \int_{\Gamma^s} \psi_i(x, y) n_x d\Gamma, \quad (57)$$

$$\psi_i(x, y) = \int N_i dx = a_{1i} x + \frac{1}{2} a_{2i} x^2 + a_{3i} y. \quad (58)$$

通过 Gauss 积分, 得

$$\tilde{N}_i = \frac{1}{A_C} \sum_{m=1}^k \sum_{n=1}^{N_G} \frac{1}{2} W_{m,n} \psi_i(x_{m,n}^{\text{GP}}, y_{m,n}^{\text{GP}}) n_x^m l_m, \quad (59)$$

$$\tilde{\mathbf{M}} = \sum_{C=1}^{N_{\text{eg}}} A_C \tilde{\mathbf{N}}_C^T \mathbf{m} \tilde{\mathbf{N}}_C. \quad (60)$$

由此, 层合板有限元控制方程中的矩阵都已沿光滑域的边界段进行光滑处理和计算, 在计算过程中不需要坐标映射和 Jacobi 矩阵的计算。

4 数值算例

下面通过数值算例分析复合材料层合板的自由振动问题。如无特殊说明, 层合板各层具有相同的厚度, 且由均匀线弹性复合材料构成, 无量纲固有频率为 $\bar{\omega} = (\omega a^2/h) \sqrt{\rho/E_2}$ 。

4.1 算例1

首先以一长度为 a 、厚度为 h 的四边简支对称层合方板 ($0^\circ/90^\circ/90^\circ/0^\circ$) 为研究对象, 探讨 RES-DSG3 法在求解复合材料动力学问题时的收敛性和有效性。对于规则网格, $\alpha=0$; 不规则网格, $\alpha=0.4$, 其中 α 为定义在区间

0~0.5的不规则系数^[20].相关的材料参数为 $E_1/E_2=10,20,30$, $G_{12}=G_{13}=0.6E_2$, $G_{23}=0.5E_2$, $\nu_{12}=0.25$, $\rho=1$,剪切修正因子 $\zeta=5/6$.

由表1可见,不同节点分布和不同弹性模量比时的四层层合板的一阶无量纲固有频率与文献[21]的一阶剪切理论的精确解很接近,具有较高的计算精度,表明了本文方法的有效性和收敛性.同时,网格“质量”对计算精度的影响很小,即使在极不规则的网格下也能获取稳定可靠的计算结果,进一步拓宽了该单元的使用范围.

表1 四层复合材料简支层合板的一阶无量纲固有频率

Table 1 The non-dimensional 1st fundamental frequency of the simply supported 4-layer laminated composite plate

number of meshes	$E_1/E_2=10$			$E_1/E_2=20$			$E_1/E_2=30$		
	$\alpha=0$	$\alpha=0.4$	ref. [21]	$\alpha=0$	$\alpha=0.4$	ref. [21]	$\alpha=0$	$\alpha=0.4$	ref. [21]
13 × 13	8.293	8.309		9.525	9.526		10.259	10.246	
15 × 15	8.293	8.306		9.535	9.528		10.275	10.255	
17 × 17	8.294	8.300	8.298	9.541	9.539	9.567	10.285	10.276	10.326
19 × 19	8.294	8.301		9.546	9.548		10.293	10.283	

4.2 算例2

考虑三层对称层合方板($0^\circ/90^\circ/0^\circ$),边长为 a ,厚度为 h ,材料参数为 $E_1/E_2=40$.采用 17×17 网格离散求解域,对不同边界条件和不同边厚比条件下的板进行了数值计算.

表2列出了通过本文方法计算的四边简支(SS),四边固支(CC),两对边简支、另两对边固支(SC)三种边界条件和不同边厚比的三层层合方板的一阶固有频率,并分别与文献[21-22]基于FSDT的复合二次径向基函数法计算的结果进行了对比,具有较好的一致性.同时,表3列出了三种边界条件下的前三阶固有频率,可以看出本文方法计算的无量纲固有频率与文献[23]基于高阶剪切变形理论计算的结果也很接近,验证了本文方法的有效性.

表2 三层复合材料层合板的一阶无量纲固有频率

Table 2 The non-dimensional 1st fundamental frequency of the 3-layer laminated composite plate

a/h	method	SS	SC	CC	a/h	method	SS	SC	CC
2	ref. [22]	5.211	5.217	5.263	10	ref. [22]	14.804	17.199	19.678
	ref. [21]	5.205	5.211	5.257		ref. [21]	14.767	17.175	19.669
	present	5.149	5.571	5.256		present	14.475	17.346	19.626
5	ref. [22]	10.207	10.658	11.274	100	ref. [22]	18.355	28.165	40.234
	ref. [21]	10.290	10.646	11.266		ref. [21]	18.891	28.501	40.743
	present	10.116	10.675	11.477		present	18.565	28.616	40.761

表3 三层复合材料层合板前三阶无量纲固有频率($a/h=10$)

Table 3 The non-dimensional 1st 3 fundamental frequencies of the 3-layer laminated composite plate ($a/h=10$)

model	method	SS	SC	CC
1	present	14.384	17.346	19.626
	ref. [23]	14.766	17.175	19.669
2	present	22.040	23.794	25.187
	ref. [23]	22.158	23.677	25.349
3	present	36.521	37.996	38.553
	ref. [23]	36.900	37.720	38.650

5 结论

本文将基于全局坐标的重构边界光滑DSG单元用于复合材料层合板的自由振动问题分析.与原始的DSG单元相比,该方法不需要对系统方程进行坐标映射,同时结合光滑技术将有限元矩阵的域积分简化为沿平滑单元边界的线积分.从数值计算结果来看,RES-DSG3法在复合材料层合板自由振动分析时表现出良好

的性能, 具有较高的计算精度; 即使是不规则网格, 也能获得较好的结果, 是一种有效可行的方法。此外, 该方法中的光滑技术也可以扩展到其他问题的有限元框架内。

参考文献(References):

- [1] 罗英勤, 李华东, 洪明. 复合材料层合板振动特性基础研究综述[J]. 复合材料科学与工程, 2020(1): 114-119. (LUO Yingqin, LI Huadong, HONG Ming. Review of the vibration characteristics of composite laminated plates[J]. *Composites Science and Engineering*, 2020(1): 114-119.(in Chinese))
- [2] 叶天贵, 靳国永, 刘志刚. 基于改进Chebyshev级数的层合结构振动分析新理论[J]. 应用数学和力学, 2019, 40(1): 58-74. (YE Tiangui, JIN Guoyong, LIU Zhigang. A new layerwise theory for vibration analysis of laminated structures based on modified Chebyshev polynomials[J]. *Applied Mathematics and Mechanics*, 2019, 40(1): 58-74.(in Chinese))
- [3] 刘旭, 姚林泉. 热环境中旋转功能梯度纳米环板的振动分析[J]. 应用数学和力学, 2020, 41(11): 1224-1236. (LIU Xu, YAO Linquan. Vibration analysis of rotating functionally gradient nano annular plates in thermal environment[J]. *Applied Mathematics and Mechanics*, 2020, 41(11): 1224-1236.(in Chinese))
- [4] 童瑶, 姚玉喆. 基于20节点辛元的复合材料层合板应力分析[J]. 应用数学和力学, 2020, 41(5): 509-516. (TONG Yao, YAO Yuzhe. 20-node hexahedron symplectic elements for stress analysis of composite laminates[J]. *Applied Mathematics and Mechanics*, 2020, 41(5): 509-516.(in Chinese))
- [5] CALIRI M F, FERREIRA A J, TITA V. A review on plate and shell theories for laminated and sandwich structures highlighting the finite element method[J]. *Composite Structures*, 2016, 156(15): 63-77.
- [6] LIU G R, DAI K Y, NGUYEN T T. A smoothed finite element method for mechanics problems[J]. *Computational Mechanics*, 2007, 39(6): 859-877.
- [7] LIU G R, NEUYEN-THOI T, NGUYEN-XUAN H, et al. A node-based smoothed finite element method (NS-FEM) for upper bound solutions to solid mechanics problems[J]. *Computers and Structures*, 2009, 87(1/2): 14-26.
- [8] LIU G R, NEUYEN-THOI T, LAM K Y. An edge-based smoothed finite element method (ES-FEM) for static, free and forced vibration analyses of solids[J]. *Journal of Sound and Vibration*, 2009, 320(4/5): 1100-1130.
- [9] NEUYEN-THOI T, LIU G R, LAM K Y, et al. A face-based smoothed finite element method (FS-FEM) for 3D linear and geometrically non-linear solid mechanics problems using 4-node tetrahedral elements[J]. *International Journal for Numerical Methods in Engineering*, 2009, 78(3): 324-353.
- [10] LEE K, SON Y, IM S. Three-dimensional variable-node elements based upon CS-FEM for elastic-plastic analysis [J]. *Computers and Structures*, 2015, 158: 308-332.
- [11] 秦剑波, 谢伟, 王峰. 基于光滑边域有限元法的二维裂纹扩展分析[J]. 应用力学学报, 2019, 36(1): 47-52, 252. (QIN Jianbo, XIE Wei, WANG Feng. An analysis of 2D crack growth based on ES-FEM[J]. *Chinese Journal of Applied Mechanics*, 2019, 36(1): 47-52, 252.(in Chinese))
- [12] NEUYEN-THOI T, PHUNG-VAN P, NGUYEN-XUAN H, et al. A cell-based smoothed discrete shear gap method using triangular elements for static and free vibration analyses of Reissner-Mindlin plates[J]. *International Journal for Numerical Methods in Engineering*, 2012, 91(7): 705-741.
- [13] 游翔宇, 郑文成, 李威, 等. 基于边光滑有限元法的加筋板静力和自由振动分析[J]. 计算力学学报, 2018, 35(1): 28-34. (YOU Xiangyu, ZHENG Wencheng, LI Wei, et al. Static and free vibration analysis of stiffened plates by ES-FEM using triangular element[J]. *Chinese Journal of Computational Mechanics*, 2018, 35(1): 28-34.(in Chinese))
- [14] NATARAJAN S, FERREIRA A J, BORDAS S P A, et al. Analysis of composite plates by a unified formulation-cell based smoothed finite element method and field consistent elements[J]. *Composite Structures*, 2013, 105: 75-81.
- [15] 林晓珊, 杨晓翔, 高剑虹. 基于扩展有限单元法的短纤维/橡胶复合材料裂纹扩展分析[J]. 固体力学学报, 2022, 43(1): 81-94. (LIN Xiaoshan, YANG Xiaoxiang, GAO Jianhong. Crack propagation analysis of short fiber reinforced rubber composites based on extended finite element method[J]. *Chinese Journal of Solid Mechanics*, 2022, 43(1): 81-94.(in Chinese))

- [16] BLETZINGER K-U, BISCHOFF M, RAMM E. A unified approach for shear-locking-free triangular and rectangular shell finite elements[J]. *Computers and Structures*, 2000, **75**(3): 321-334.
- [17] NGUYEN-XUAN H, LIU G R, THAI-HOANG C, et al. An edge-based smoothed finite element method (ES-FEM) with stabilized discrete shear gap technique for analysis of Reissner-Mindlin plates[J]. *Computer Methods in Applied Mechanics and Engineering*, 2010, **199**(9/12): 471-489.
- [18] NGUYEN-XUAN H, RABCZUK T, NGUYEN-THANH N, et al. A node-based smoothed finite element method with stabilized discrete shear gap technique for analysis of Reissner-Mindlin plates[J]. *Computational Mechanics*, 2010, **46**(5): 679-701.
- [19] YANG G, HU D A, LONG S Y. A reconstructed edge-based smoothed DSG element based on global coordinates for analysis of Reissner-Mindlin plates[J]. *Acta Mechanica Sinica*, 2017, **33**: 83-105.
- [20] LIU G R, DAI K Y, NGUYEN T T. A smoothed finite element method for mechanics problems[J]. *Computational Mechanics*, 2007, **39**: 859-877.
- [21] REDDY J N. *Mechanics of Laminated Composite Plates and Shells: Theory and Analysis*[M]. Boca Raton: CRC Press, 1997.
- [22] FERREIRA A, ROQUE C, JORGE R. Free vibration analysis of symmetric laminated composite plates by FS-DT and radial basis functions[J]. *Computer Methods in Applied Mechanics and Engineering*, 2005, **194**(39/41): 4265-4278.
- [23] KHDEIR A A, LIBRESCU L. Analysis of symmetric cross-ply laminated elastic plates using a higher-order theory part II: buckling and free vibration[J]. *Composite Structures*, 1988, **9**(4): 259-277.